

Research Paper

Structural characterization of the complex of the Rev response element RNA with a selected peptide

Qing Zhang ^a, Kazuo Harada ^b, Ho S. Cho ^a, Alan D. Frankel ^b,
David E. Wemmer ^{a, *}

^aDepartment of Chemistry MC-1460, University of California, and Physical Biosciences, Division, Lawrence Berkeley National Laboratory, Berkeley, CA 94720, USA

^bDepartment of Biophysics and Biochemistry, University of California, San Francisco, CA 94143-0448, USA

Received 12 December 2000; revisions requested 13 February 2001; revisions received 14 March 2001; accepted 16 March 2001
First published online 30 March 2001

Abstract

Introduction: The RSG-1.2 peptide was selected for specific binding to the Rev response element RNA, as the natural Rev peptide does. The RSG-1.2 sequence has features incompatible with the helical structure of the bound Rev peptide, indicating that it must bind in a different conformation.

Results: The binding of the RSG-1.2 peptide to the Rev response element RNA was characterized using multinuclear, multidimensional NMR. The RSG-1.2 peptide is shown to bind with the N-terminal segment of the peptide along the major groove in an extended conformation and turn preceding a C-terminal helical segment, which crosses the RNA groove in the region

widened by the presence of purine–purine base pairs. These features make the details of the bound state rather different than that of the Rev peptide which targets the same RNA sequence binding as a single helix along the groove axis.

Conclusions: These studies further demonstrate the versatility of arginine-rich peptides in recognition of specific RNA elements and the lack of conserved structural features in the bound state. © 2001 Elsevier Science Ltd. All rights reserved.

Keywords: Peptide–RNA complex; RNA recognition; Selected peptide; Solution structure

1. Introduction

RNA–protein interactions participate in a wide variety of biological functions and utilize a diverse set of protein and RNA structural motifs for sequence-specific recognition (see [1–6] for recent reviews). Among the most common protein motifs used to bind RNA are the RNP (or RRM or RBD) domain, KH domain, zinc finger, double-stranded RNA-binding domain (dsRBD), and the arginine-rich motif (ARM). Most of these domains are stably folded in the absence of RNA, and each class of protein appears to interact with RNA in a relatively conserved way. For example, members of the RNP class all use a β -sheet platform to bind RNA, though the detailed structures of their RNA-binding sites differ substantially. In contrast, arginine-rich domains, which typically are less

than 20 amino acids in length, often are unstructured or form marginally stable secondary structures in the absence of RNA and have been observed to adopt α -helical, bent helical, β -hairpin, and extended conformations upon RNA binding (see [7–9] for recent reviews). In these cases, it has been hypothesized that the RNA framework provides a scaffold that helps establish the fold of the polypeptide. Indeed, it recently has been shown that an arginine-rich peptide from the HIV-1 Rev protein adopts two different conformations (α -helical or extended) when bound in the context of two different RNA aptamers [10].

The ARM initially was discovered in bacteriophage anti-terminator proteins, viral regulatory proteins, viral coat proteins, and ribosomal proteins [11]. Studies with short peptides showed that these regions alone often can bind to their RNA sites with high affinity and specificity and provide good models of their corresponding RNA–protein interactions (see [7–9]). While it may have been anticipated that basic peptides would bind RNA with high affinity based on the potential for electrostatic interactions, the relatively high binding specificity was not an-

* Correspondence: David E. Wemmer;
E-mail: dewemmer@lbl.gov

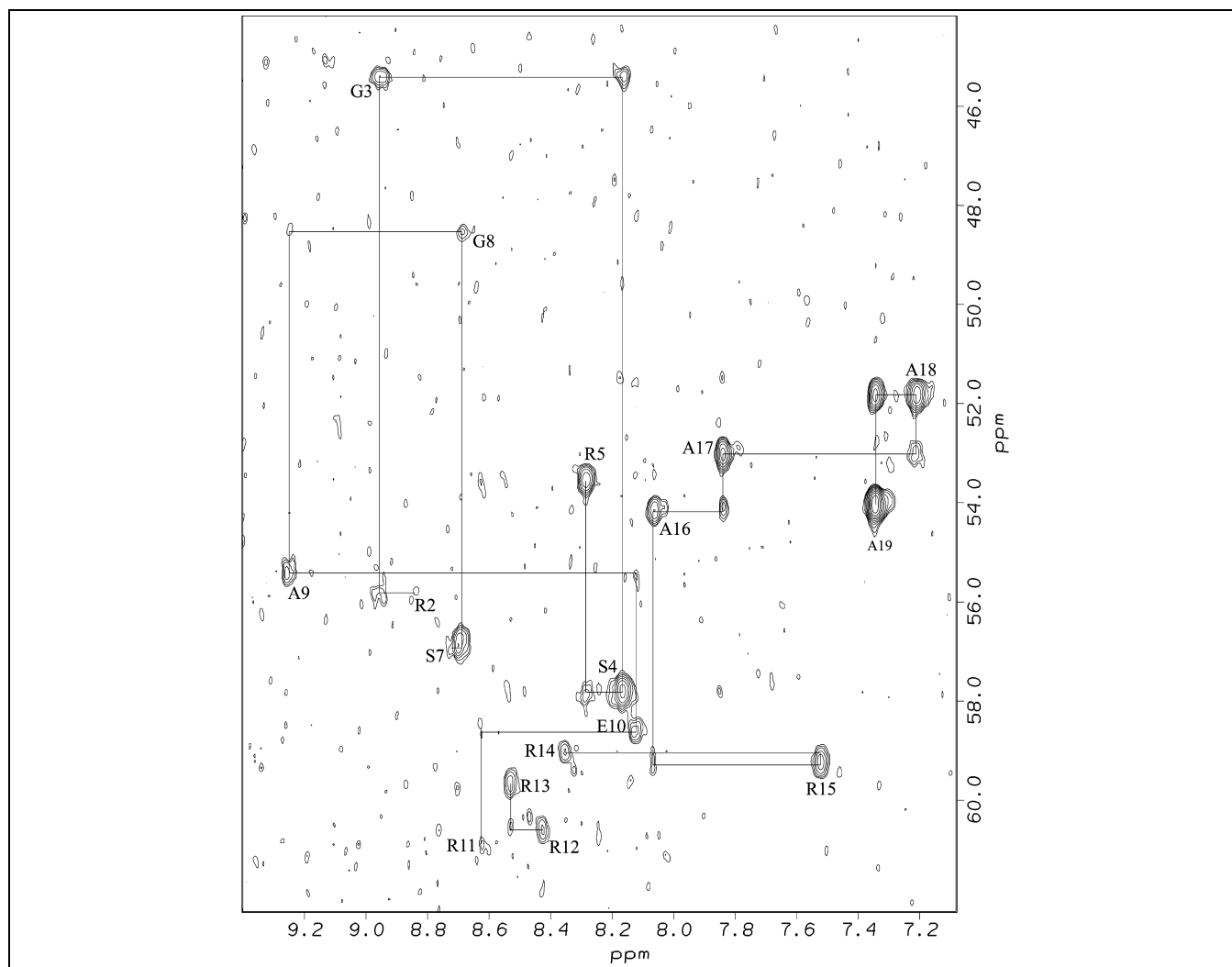


Fig. 2. 2D HNCA spectrum of ^{13}C , ^{15}N labeled peptide in complex with unlabeled RRE RNA. Intra-residue peaks are labeled with the residue number, and horizontal lines indicate interresidue connectivities. Weak connectivities were verified in other experiments.

and 8.46 ppm, NHs which belong to Arg and/or Ala residues. Because of the poor dispersion in proton chemical shifts and apparent lack of structure, the free peptide was not characterized in any further detail.

The assignments of the peptide NMR signals in the complex were started from the 100 ms mixing time 3D HSQC-NOESY and 2D HNCA experiments. Fig. 2 shows the constant-time HNCA spectrum for the unlabeled RNA/ ^{15}N , ^{13}C -labeled peptide complex. The numbers indicate intranucleotide NH to C_α crosspeaks. The solid lines show the connectivities from Arg2 to Arg5, Ser7 to Arg11 and Arg14 to Ala19. There are two breaks in the connectivities, one is from Arg11 to Arg12, and the other from Arg13 to Arg14. Arg12 and Arg13 had a weak connection in the HNCA experiment, but this, taken with the residue identification from TOCSY and NOESY data, and the ^{15}N resolved NOESY made the assignments clear.

The 3D HSQC-NOESY (50 ms and 100 ms mixing times) experiments were also used to verify assignments, and volumes of NOE crosspeaks in the 50 ms mixing time

HSQC-NOESY experiment were integrated to extract distance restraints. Fig. 3 shows a strip plot of the 50 ms mixing time HSQC-NOESY experiment for the unlabeled RNA/ ^{15}N -labeled peptide complex. Sequential $\text{NH}(i)$ to $\text{NH}(i+1)$ backbone NOEs were observed from residue Gly8 through Ala19, and between Gly3 and Ser4, but not between other adjacent residues. $\text{NH}(i+3)$ to H_α NOE crosspeaks were observed for residues between Arg12 and Ala19, but the Arg14 NH to Arg11 α proton NOE crosspeak was only seen in a 100 ms HSQC-NOESY experiment. In addition, small $\text{HN}-\text{H}_\alpha$ coupling constants (~ 5 Hz) were observed in an HMQC-J experiment. Deviations of α -proton and α -carbon chemical shifts from random coil (defining a chemical shift index, [16,17]) indicate that the peptide residues Glu10 to Ala17 are helical. Other regions of the peptide do not appear to have regular secondary structure. An NOE crosspeak from Ser7 NH to Glu10 NH was observed in both 50 ms and 100 ms HSQC-NOESY experiments. The NHs of Ser7 and Glu10 also see several protons in common above 5 ppm,

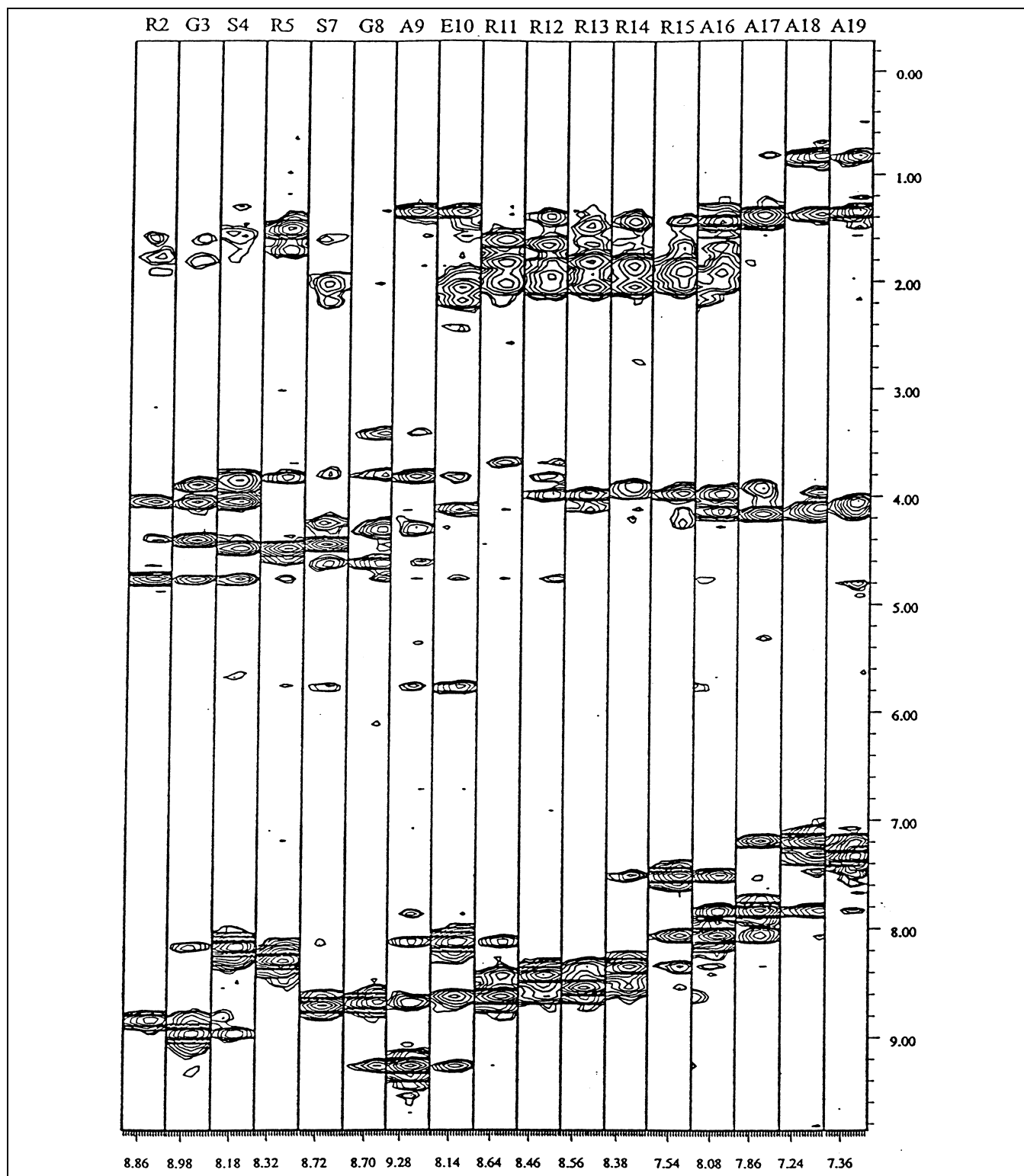


Fig. 3. A strip plot representation of sections of the 3D ^{15}N HSQC NOESY spectrum of ^{15}N labeled peptide in complex with unlabeled RNA is shown. The residue assignments are indicated at the top of each strip, the chemical shift of the strip is shown at the bottom.

indicating that these two NHs are close in space, requiring some sort of turn. In the 50 ms homonuclear NOESY spectrum, NOE crosspeaks were observed from the Arg5 α -proton to both δ -protons of Pro6. This indicates that

the Pro6 amide is in the trans-conformation, which is further supported by the chemical shift of Pro6 $\text{C}\alpha$ (62.2 ppm). The HCCH-COSY and HCCH-TOCSY experiments were performed to help assign peptide sidechains.

Table 1

| | |
|--|---------------|
| Intra-RNA restraints | 620 |
| Intrapeptide restraints | 99 |
| Intermolecular restraints | 8 |
| r.m.s. distance restraint violation | 0.03 Å |
| Largest violation | 0.10 Å |
| r.m.s. angle constraint violation | 1.22° |
| Largest angle constraint violation | 2.5° |
| Structure r.m.s.d.s (backbone heavy atoms) | |
| Complex (RNA 5–13, 20–30+peptide) | 1.53 ± 0.65 Å |
| Complex (all residues) | 2.45 ± 0.75 Å |
| RNA (5–13, 20–30) | 1.33 ± 0.42 Å |
| Peptide (all residues) | 1.14 ± 0.28 Å |

For the RRE IIB RNA hairpin (Fig. 1), sequential imino–imino NOE crosspeaks were observed in the H₂O NOESY for most of the helical segments, in analogy to the Rev/RRE complex [18]. No imino–imino connectivity was observed from U45 to G46, or from U66 to G67, due to the long distance between imino–imino protons of 5'-UG-3'. The connectivity between G50 and G70 was also missing. However, the NOE crosspeak between the imino protons of G50 and G67 helped to assign them, with the assignment of the G50 imino proton confirmed from the aromatic region of the RNA.

The aromatic to H1' crosspeak regions of the D₂O NOESYs of the complex were used, together with heteronuclear NMR experiments, to assign aromatic and H1' resonances. The HMQC experiments helped with unambiguous assignments of AH2s and C and U H5s, since these carbons have distinct chemical shifts. The long-range HSQC experiment [19] helped with making connections between aromatic protons and sugar protons. Fig. 4 shows the sequential NOE pathway finally determined for the RRE RNA. The sequential NOE connectivities observed for the RRE RNA bound to RSG-1.2 peptide are quite similar to those for the RRE RNA bound to the wild-type Rev peptide. The sequential *i*, *i*–1 NOEs from H8/H6 protons to H1' protons of the 5' neighboring nucleotide were observed along almost the entire length of the RNA, with two breaks: one at A68, and the other at U72. For these breaks, the *i*, *i*–2 NOEs from C69 to G67 and A73 to G71 were observed, although in crowded regions. This pattern is consistent with the unstacking of A68 and U72 as single nucleotide bulges, consistent with the fact that the U72 imino proton is not seen in the H₂O NOESY. The same NOE connectivity and similar chemical shifts were observed for the GCAA loop as reported in previous work [20]. Sequential NOE connectivities were also observed for the single stranded segment of the RNA from G80 to U83, and U84 was assigned by its sharp lines.

Upon binding to the RSG-1.2 peptide, two Watson–Crick base pairs are formed (G50•C69 and C49•G70) and two non-Watson–Crick base pairs are formed (G48•G71 and G47•A73), as observed for wild-type Rev peptide [18]. The sharp imino resonances observed for the internal loop indicate that binding of the peptide stabilizes

the internal loop imino protons from exchange with water. A strong G48–G71 imino–imino NOE provides direct evidence for the symmetric G48•G71 base pair formation, and a strong G47 imino to A73H2 NOE indicates the formation of a G47•A73 base pair in the complex. The binding site can be roughly identified from the chemical shift differences between the imino protons of the free RRE RNA and the complexed RNA, and spans from the A52–U66 base pair to G46–A75.

Contacts between the RNA and peptide were observed primarily in double-half-filtered NOESYs (mixing times of 50 ms and 150 ms) performed on the unlabeled RNA/¹³C,¹⁵N-labeled peptide complex. Non-exchangeable protons on three residues of the peptide have NOE connections to the RNA. At 50 ms mixing time, Ala18 βH and A68 H1' gave a strong NOE crosspeak. At 150 ms mixing time, Ala18 βH gave a medium to strong crosspeak with A68 H2 and a strong crosspeak with A68 H1', and Ala18 αH also gave a weak to medium crosspeak with A68 H2. A strong NOE crosspeak was seen between the Ala9 methyl group and RNA U45 H5 at both 50 ms and 150 ms. At 150 ms mixing time, the Ala9 methyl group also gave weak to medium NOE crosspeaks with U45 H6 and G46 H8. The Arg2 sidechain protons (δ, γ, β, α) showed weak to medium NOE crosspeaks with U66 H5 at 150 ms mixing time. At 50 ms mixing time, these crosspeaks were very weak or missing altogether. There were a number of crosspeaks observed involving exchangeable protons in NOESY data from H₂O solutions, however these could not be unambiguously assigned and hence were not used in the structure determination of the complex.

For calculations of the structure of the complex the helical regions of RNA were constrained to an A-form, while other regions were constrained just with experimental distances giving a total of 620 intra-RNA constraints. In addition 99 intrapeptide experimentally determined constraints used together with the observed eight intermolecular contacts. After calculating the structure with DYANA, and carrying out energy minimization with OPAL, the structures of the peptide and RNA are reasonably well defined, as are their relative positions (Fig. 5A). Since there are a substantial number of NOEs defining the helical, C-terminal portion of the peptide it is not surprising that it overlays more precisely (0.48 ± 0.23 Å r.m.s.d.) than the full peptide (1.14 ± 0.28 Å r.m.s.d.). The overall RNA is also locally fairly well defined (giving 1.33 ± 0.42 Å r.m.s.d. for the region near the peptide, residues 5–13 and 20–30), however long-range variation such as bending is seen among the structures (for all residues 2.45 ± 0.75 Å r.m.s.d.). The contacts between peptide and RNA are sufficient to define their relative positions, with all structures indicating that the helical segment of the peptide crosses the groove, and that the N-terminal portion of the peptide extends along the RNA toward the hairpin loop, although the local conformation of that portion of the peptide is not precisely defined. The peptide plus RNA in the con-

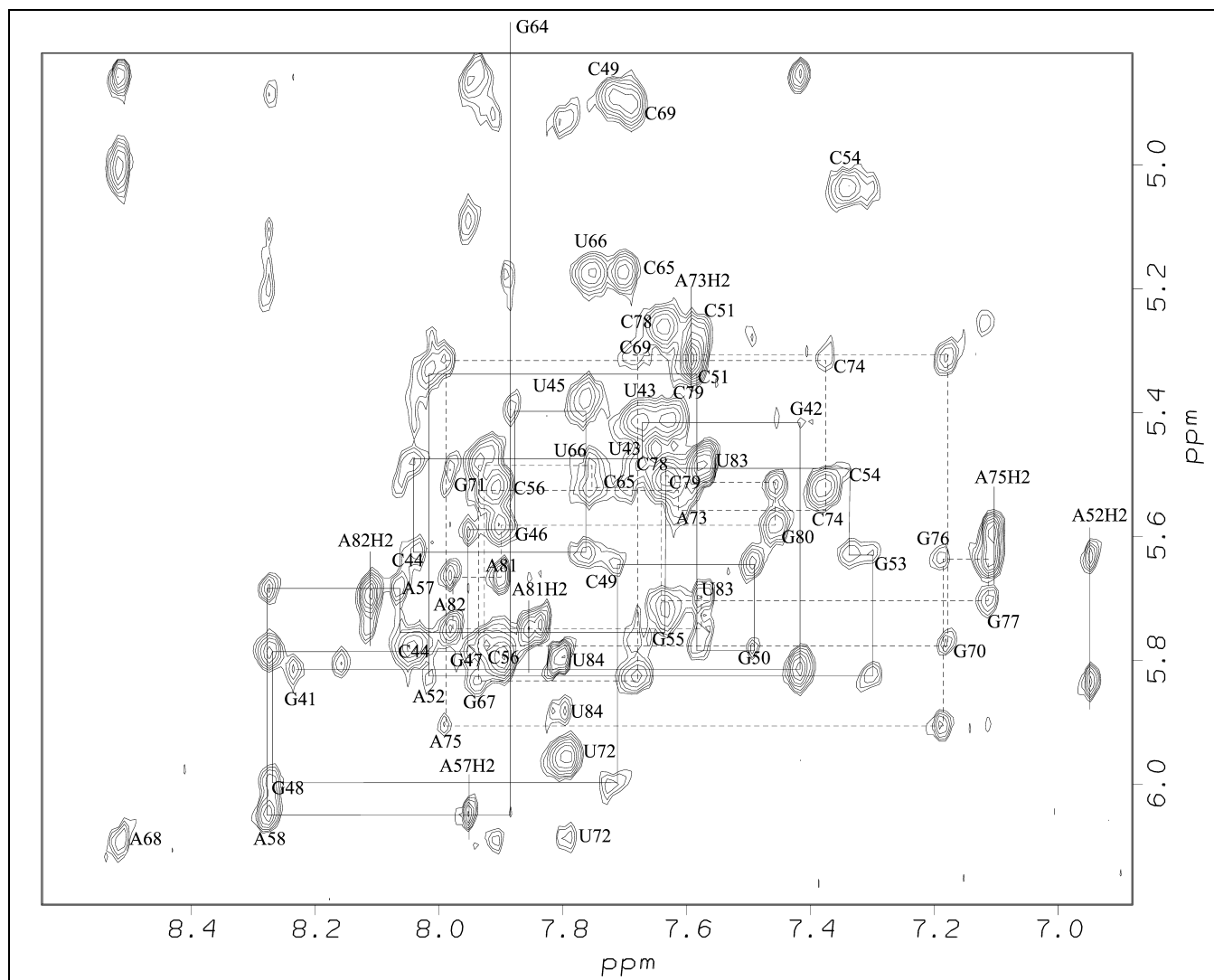


Fig. 4. The aromatic to H1' crosspeak region of unlabeled RRE RNA in complex with unlabeled peptide is shown. Connectivities for the 5' segment of the hairpin (residues 41–64) are indicated by solid lines and the 3' segment (residues 65–83) by dashed lines. Intra-residue connectivities are indicated with the residue identity and number.

tacted region gives a 1.53 ± 0.65 Å r.m.s.d. The r.m.s.d. values for the peptide are higher when sidechains are included since few of the sidechains have conformations defined by the data. The data for the structure are summarized in Table 1. The coordinates for the seven energy minimized models have been deposited in the RCSB database under entry 1IqF.

3. Discussion

The Rev peptide when bound to the RRE adopts a helical conformation throughout the peptide, with the N-terminus of the peptide binding deep in the major groove of the RNA (Fig. 5C). The specificity of the Rev peptide for the RNA target arises both through structure-specific interactions (two purine–purine pairs widening the minor groove to allow the helix to fit), and sequence specific

contacts (arginine sidechains contacting the edges of bases presented by the induced RNA structure, and a key asparagine hydrogen bonding to the G•A base pair induced in the bound structure). The binding of the RSG-1.2 peptide has some features in common, but many differences as well. While the Rev peptide is helical throughout, only residues 9–17 of RSG-1.2 are helical in its complex (Fig. 5B). The helix ends at Gly8, which is not surprising as it is the last of three consecutive helix breaking residues. From Ser4 through Gly8 the backbone is in an extended conformation. The single NH to NH NOE between residues Gly3 and Ser4 indicates an irregular turn, with Arg1 and Arg2 again extended. The sequential NOEs are supported by the chemical shifts for the $^{13}\text{C}_\alpha$ and H_α , which also indicate helix for residues 9–17, and an extended conformation for residues 4, 5, and 7 with coil for the remainder, this region being quite variable among the calculated structures.

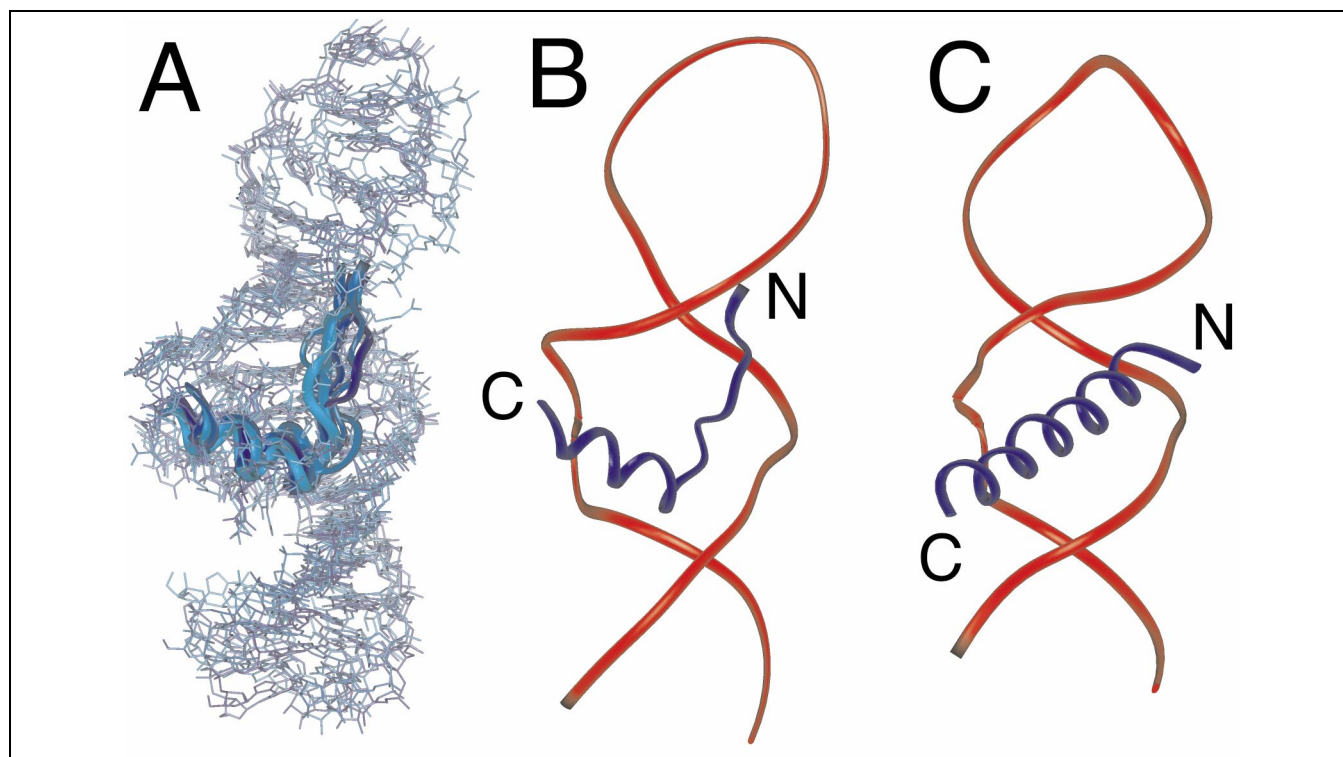


Fig. 5. (A) The family of seven computed structures of the RSG-1.2 peptide RRE RNA complex is shown at the left with the RNA represented just by heavy atoms and the peptide as a ribbon. (B) One structure of the seven presented in (A), shown in ribbon format for both the peptide and RNA. (C) One structure of the Rev peptide bound to the RRE RNA (from pdb file1ETG) shown in ribbon format for peptide and RNA to be compared with (B).

The binding of the Rev peptide to the RRE alters the structure of the RNA, inducing specific base pairing in the internal loop region, including the G47•A73 and G48•G71 pairs which lead to a widening of the groove that appears critical for the binding of Rev. The binding of the RSG-1.2 peptide seems to induce very similar structure in the RRE, specifically including the purine pairs. The similarity of the RRE structure, in spite of differences in the peptide structure indicates that the RNA structure is probably driven more by the need for a widened groove to accommodate the peptide than by the sequence-specific interactions, which must be quite different in the two complexes. This RNA also contains single base bulges at residues A68 and U72. The NOE patterns at these residues suggest that these are looped out in the peptide-bound structure, since stacking of bases above and below these nucleotides is seen.

Although the number of intermolecular contacts which we have identified is small, taken together with the features of the peptide secondary structure they define the position of the peptide on the RNA relatively well. A number of NOEs are observed between C-terminal residues of the peptide, Ala18 and Arg15, and the looped out base A68. The upfield shift of the Ala18 methyl is consistent with a ring current from a base such as A68. At the other end of the helical peptide segment there are contacts observed between Ala9 and bases U45, G46 and

G47. These contacts show that the helix lies across the groove to a much larger extent than the Rev peptide, for which the axis of the peptide helix lies along the groove. Ala9 was identified in the peptide selection as an important residue for binding [12]. Beyond Ala9, contacts are observed between Ser7 and G46 and G47, and then between Arg2 and U66 or C65. These are consistent with the extended peptide conformation, determined by intrapeptide NOEs, indicating that the peptide chain extends up along the RNA groove. The contacts to the alanine residues likely reflect hydrophobic interactions, which contribute to the specificity in binding. However the lack of assignments of the polar sidechain-exchangeable protons, particularly of arginine, prevents identification of other particular interactions which must also contribute to specificity. In our structures the sidechains are localized to some extent by the defined backbone conformation, however the contacts made are variable and do not indicate the extent to which binding is sequence specific rather than structure specific. Certainly the peptide could not bind in an equivalent way to a standard A-form RNA helix, as is true for the native Rev peptide where the widening of the groove is critical to forming the correctly shaped binding pocket. In the binding mode for the RSG-1.2 peptide described, shape discrimination may be even more important and may contribute to the specificity for binding to the RRE RNA sequence.

Despite the fact that both the Rev and RSG-1.2 peptides are arginine-rich, they bind very differently to the same RNA target (compare Figs. 5B and 5C). This reinforces the notion that sequence and even structural elements can be utilized by peptides in diverse ways to target specific sequences and structures.

While this work was in review a manuscript describing results on a very closely related peptide–RNA complex appeared [31]. Conclusions regarding the regions of helical and extended conformation of the peptide are the same, as is the overall position of the peptide. However in their work Gosser et al. were able to assign a large number of sidechain resonances and define many more contacts between peptide and RNA defining the overall structure with higher precision.

4. Materials and methods

4.1. Sample preparation

4.1.1. RNA

The fragment of HIV-1 RRE RNA used for this work (the high affinity IIB hairpin; Fig. 1, [18]) was synthesized by in vitro transcription using T7 RNA polymerase [21] and a plasmid DNA template [22]. The plasmid was linearized with *EcoRI*, which effectively adds the five nucleotides 5'-GAAUU-3' to the 3' end of the desired RNA fragment [18]. Both ^{15}N -labeled and $^{13}\text{C},^{15}\text{N}$ -labeled RNAs were made using the same procedure. The ^{15}N -labeled and $^{13}\text{C},^{15}\text{N}$ -labeled nucleotides were made using RNA isolated from large-scale cultures of *Methylophilus methylotrophus* [23]. Each ml of transcription reaction generated approximately 10 ODs of both unlabeled and uniformly labeled RNA.

4.1.2. Peptide

Labeled RSG-1.2 peptide (see Fig. 1) was made using the TrpE leader fusion system [24,25]. A DNA fragment encoding the peptide was cloned into a plasmid expressing the TrpE leader fragment with a His tag. The fusion peptide was expressed in *Escherichia coli* grown either on normal LB medium to produce unlabeled peptide, or on minimal growth medium including ^{15}N ammonium chloride and ^{13}C glucose. Expression was induced by addition of isopropylthiogalactoside (IPTG) to 5 mM, cells were grown for 4 h, and then harvested by centrifugation. After sonication and centrifugation, the fusion protein was purified by loading onto a Ni–NTA column, washing with 6 M GuHCl/0.1 M NaPO₄/0.01 M Tris pH 8.0, and then eluting with 6 M GuHCl/0.1 M NaPO₄/0.01 M Tris, pH 6.3. The resulting protein appeared as a single band on a SDS gel. The purified fusion peptide was treated with cyanogen bromide (CNBr), which cleaves the amide bond following methionine residues. CNBr cleavage was performed for 13–16 h under acidic conditions in the dark to avoid side reactions, and the mixture was then dried to remove HBr. The peptide was purified by high performance liquid chromatography (HPLC). After optimizing conditions for each step, a 500-ml M9 culture yielded 3.39 mg unlabeled peptide,

and two 300-ml cultures yielded 0.86 mg ^{15}N -labeled peptide and 0.90 mg $^{13}\text{C},^{15}\text{N}$ -labeled peptide. The identity and purity of these peptides were determined by mass spectroscopy.

4.1.3. NMR

To prepare the peptide–RNA complex, peptide was titrated into an RNA solution in approximately 0.25 mol equivalents per addition, monitoring the 1D ^1H NMR spectra (600 MHz). In the imino proton region, addition of peptide led to new resonances in slow exchange with the free RNA, replacing the free RNA spectrum completely at 1:1 stoichiometry. After the titration, the sample was lyophilized to dryness. For NMR experiments in H₂O the complex was redissolved in a 90% H₂O/10% D₂O mixture to a final volume of 160 μl (1.6 mM RNA/peptide, 20 mM sodium phosphate, pH 6.5, 100 mM sodium chloride, 0.1 mM EDTA). For experiments carried out in D₂O the solid was lyophilized twice from 99.9% D₂O (Cambridge Isotope Laboratories) and redissolved in 160 μl 99.96% D₂O (Cambridge Isotope Laboratories). Selectively labeled samples were made using the same method, with a total of seven samples used for data collection. The samples were: unlabeled RRE RNA/unlabeled peptide, ^{15}N -labeled RRE RNA/unlabeled peptide, ^{13}C and ^{15}N -labeled RRE RNA/unlabeled peptide, unlabeled RRE RNA/ ^{15}N -labeled peptide, unlabeled RRE RNA/ ^{13}C and ^{15}N -labeled peptide, free RRE RNA, and free peptide.

Homonuclear NMR experiments were performed on unlabeled free RRE RNA, free peptide, and unlabeled complex, including 2D NOESY, COSY and TOCSY experiments in both D₂O and H₂O. In addition D₂O NOESY experiments for the unlabeled RNA/unlabeled peptide sample were performed at different temperatures (15, 25 and 35°C), in order to resolve some of the overlaps. A ROESY experiment (300 ms mixing time) was also performed for the free peptide. The assignments for the RRE RNA and the RSG-1.2 peptide in the complex required the use of isotope labeling and heteronuclear NMR experiments. ^{13}C -HMQC and ^{15}N -HSQC spectra were taken at 5, 15, 25, 35, and 45°C. The best dispersion and linewidths were at 25°C, and all further heteronuclear experiments were taken at this temperature.

4.2. Restraints and structure calculations

Upper distance restraints for the peptide were calculated from 3D HSQC-NOESY (H₂O data of 50 ms mixing time and D₂O data of 80 ms mixing time) crosspeak volumes using the CALIBA procedure [26]. Backbone ϕ torsion angle restraints were determined from coupling constants and upper distance restraints using the HABAS procedure [27]. 99 distance restraints and 90 torsion angle restraints were used for the peptide in structural calculations.

The RRE RNA is mostly A-form duplex when bound to the RSG-1.2 peptide, since the sequential $i, i-1$ NOEs from H8/H6 protons to H1' protons of the 5' neighboring nucleotide were observed along almost the entire length of the RNA. Since data to obtain torsional restraints were not collected, the duplex regions of the RNA included restraints to constrain it as standard

A-form during calculations of the RNA/peptide structure. In addition the GCAA loop was constrained based on previous work [20]. Based on NOESY crosspeaks from data in H₂O, base pair hydrogen bonds were included as distance restraints between the proton and hydrogen bond acceptor using upper and lower bounds of 1.70–2.20 Å.

DQF-COSY spectra provide information about sugar puckers. Nucleotides with a H1'–H2' coupling constant of > 8 Hz in the COSY spectrum were classified as C2'-endo. Nucleotides with no COSY or TOCSY crosspeak between the H1'–H2' proton ($J < 3$ Hz) were classified as C3'-endo. Some nucleotides had weak H1'–H2' crosspeaks in the TOCSY spectrum, but no COSY crosspeaks. These are most likely nucleotides with some mixed population of C2'/C3'-endo conformations, and no torsion restraints were used for these residues. Torsional restraints were applied during restrained molecular dynamics based on these observations, using a 20° range around the standard values [28].

Initial structural calculations were performed using three intermolecular distance restraints, all derived from a 50-ms mixing time double-half-filtered NOESY experiment. The upper limit of the distance restraint between RNA A68 H1' and peptide A18 methyl group was set to 4.00 Å, that between RNA U45 H5 and peptide A9 methyl group was set to 3.00 Å, and that between RNA U66 H5 and peptide R2 αH was set to 5.00 Å.

The structure calculations were performed using simulated annealing in torsion angle space as implemented in the program DYANA [29]. 20 structures were generated with random coil starting structures for both RNA and peptide. The seven lowest target value structures among these were further energy refined using OPAL [30]. The r.m.s.d. values are computed to the mean structure of these seven, calculated using MOLMOL.

Acknowledgements

This work was supported by the Director, Office of Biological and Environmental Research, Office of Energy Research of the US Department of Energy under Contract No. DE-AC03-76SF00098, and through instrumentation Grants from the US Department of Energy, DE FG05-86ER75281, and the National Science Foundation, DMB 86-09305 and BBS 87-20134 (D.E.W.) and by Grants GM47478 and GM56531 (A.F.) and GM43129 (D.W.) from the National Institutes of Health.

References

- [1] D.E. Draper, Themes in RNA–protein recognition, *J. Mol. Biol.* 293 (1999) 255–270.
- [2] S. Cusack, RNA–protein complexes, *Curr. Opin. Struct. Biol.* 9 (1999) 66–73.
- [3] T.A. Steitz, RNA recognition by proteins, in: R.F. Gesteland, T.R. Cech, J.F. Atkins (Eds.), *The RNA World*, 2nd edn., Cold Spring Harbor Laboratory Press, Cold Spring Harbor, NY, 1999, pp. 427–450.
- [4] H. Siomi, G. Dreyfuss, RNA-binding proteins as regulators of gene expression, *Curr. Opin. Genet. Dev.* 7 (1997) 345–353.
- [5] T. Hermann, J.D. Patel, Stitching together RNA tertiary architectures, *J. Mol. Biol.* 294 (1999) 829–849.
- [6] T. Hermann, E. Westhof, Non-Watson–Crick base pairs in RNA–protein recognition, *Chem. Biol.* 6 (1999) R335–R343.
- [7] D.J. Patel, Adaptive recognition in RNA complexes with peptides and protein modules, *Curr. Opin. Struct. Biol.* 9 (1999) 75–87.
- [8] N. Narayana, M.A. Weiss, RNA recognition by arginine-rich peptide motifs, *Biopolymers* 48 (1999) 167–180.
- [9] A.D. Frankel, Fitting peptides into the RNA world, *Curr. Opin. Struct. Biol.* 10 (2000) 332–340.
- [10] X. Ye, A. Gorin, R. Frederick, W. Hu, A. Majumder, W. Xu, G. McLendon, A. Ellington, D.J. Patel, RNA architecture dictates the conformations of a bound peptide, *Chem. Biol.* 6 (1999) 657–669.
- [11] D. Lazinski, E. Grzadzińska, A. Das, Sequence-specific recognition of RNA hairpins by bacteriophage antiterminators requires a conserved arginine-rich motif, *Cell* 59 (1989) 207–218.
- [12] K. Harada, S.S. Martin, A.D. Frankel, Selection of RNA-binding peptides in vivo, *Nature* 380 (1996) 175–179.
- [13] K. Harada, S.S. Martin, R. Tan, A.D. Frankel, Molding a peptide into an RNA site by in vivo peptide evolution, *Proc. Natl. Acad. Sci. USA* 94 (1997) 11887–11892.
- [14] J.L. Battiste, H. Mao, N.S. Rao, R. Tan, D.R. Muhandiram, L.E. Kay, A.D. Frankel, J.R. Williamson, Alpha helix major groove recognition in an HIV-1 Rev peptide–RRE RNA complex, *Science* 273 (1996) 1547–1551.
- [15] R. Tan, A.D. Frankel, Costabilization of peptide and RNA structure in an HIV Rev peptide–RRE complex, *Biochemistry* 33 (1994) 14579–14585.
- [16] D.S. Wishart, B.D. Sykes, The ¹³C chemical-shift index: a simple method for the identification of protein secondary structure using ¹³C chemical-shift data, *J. Biomol. NMR* 4 (1994) 171–180.
- [17] D.S. Wishart, B.D. Sykes, F.M. Richards, The chemical shift index: a fast and simple method for the assignment of protein secondary structure through NMR spectroscopy, *Biochemistry* 31 (1992) 1647–1651.
- [18] J.L. Battiste, R. Tan, A.D. Frankel, J.R. Williamson, Binding of an HIV Rev peptide to Rev responsive element RNA induces formation of purine–purine base pairs, *Biochemistry* 33 (1994) 2741–2747.
- [19] V. Sklenar, R.D. Peterson, M.R. Rejante, J. Feigon, Correlation of nucleotide base and sugar protons in a ¹⁵N-labeled HIV-1 RNA oligonucleotide by ¹H-¹⁵N HSQC experiments, *J. Biomol. NMR* 4 (1994) 117–122.
- [20] F.M. Jucker, H.A. Heus, P.F. Yip, E.H. Moors, A. Pardi, A network of heterogeneous hydrogen bonds in GNRA tetraloops, *J. Mol. Biol.* 264 (1996) 968–980.
- [21] J.F. Milligan, D.R. Groebe, G.W. Witherell, O.C. Uhlenbeck, Oligoribonucleotide synthesis using T7 RNA polymerase and synthetic DNA templates, *Nucleic Acids Res.* 15 (1987) 8783.
- [22] G. Varani, F. Aboul-ela, F.H.-T. Allain, NMR investigation of RNA structure, *Prog. Nuclear Magn. Reson. Spectrosc.* 29 (1996) 51–127.
- [23] R.T. Batey, N. Cloutier, H. Mao, J.R. Williamson, Improved large scale culture of *Methylophilus methylotrophus* for ¹³C/¹⁵N labeling and random fractional deuteration of ribonucleotides, *Nucleic Acids Res.* 24 (1996) 4836–4837.
- [24] T.N.M. Schumacher, L.M. Mayr, D.L. Minor Jr., M.A. Milhollen, M.W. Burgess, P.S. Kim, Identification of D-peptide ligands through mirror-image phage display, *Science* 271 (1996) 1854–1857.
- [25] J.P. Staley, P.S. Kim, Formation of a native-like subdomain in a partially folded intermediate of bovine pancreatic trypsin inhibitor, *Protein Sci.* 3 (1994) 1822–1832.
- [26] P. Güntert, W. Braun, K. Wüthrich, Efficient computation of three-dimensional protein structures in solution from nuclear magnetic resonance data using the program DIANA and the supporting programs CALIBA, HABAS and GLOMSA, *J. Mol. Biol.* 217 (1991) 517–530.

- [27] P. Güntert, W. Braun, M. Billeter, K. Wüthrich, Automated stereospecific ^1H NMR assignments and their impact on the precision of protein structure determinations in solution, *J. Am. Chem. Soc.* 111 (1989) 3997–4004.
- [28] W. Saenger, *Principles of Nucleic Acid Structure*, Springer, New York, 1984.
- [29] P. Güntert, C. Mumenthaler, K. Wüthrich, Torsion angle dynamics for NMR structure calculation with the new program DYANA, *J. Mol. Biol.* 273 (1997) 283–298.
- [30] P. Luginbühl, P. Güntert, M. Billeter, K. Wüthrich, The new program OPAL for molecular dynamics simulations and energy refinements of biological macromolecules, *J. Biomol. NMR* 8 (1996) 136–146.
- [31] Y. Gosser, T. Hermann, A. Majumdar, W. Hu, R. Frederick, F. Jiang, W. Xu, D.J. Patel, Peptide-triggered conformational switch in HIV-1 RRE RNA complexes, *Nat. Struct. Biol.* 8 (2001) 146–150.